Training toward Advanced 3D Seismic Methods for CO2 Monitoring, Verification, and Accounting

Type of Report: Progress

Frequency of Report: Quarterly

Reporting Period: Jan. 1, 2011 – Mar 31, 2011

DOE Award Number: DE-FE002186 (UH budget G091836)

Submitting Organizations: Department of Earth and Atmospheric Sciences
Allied Geophysical Lab
University of Houston
Houston, Texas 77004-5505

Preparers: Prof. Christopher Liner – P.I.
Phone: (713) 743-9119
Fax: (713) 748-7906
Dr. Jianjun Zeng (research scientist)
Qiong Wu (PHD candidate) … coordinator for this report
Johnny Seales (undergraduate)
Shannon Leblanc (MS candidate)
Bryan Flynn (MS candidate)

Distribution List:

FITS	FITS@netl.doe.gov	DOE-NETL
Karen Cohen	Karen.Cohen@netl.doe.gov	DOE-NETL
Vanessa Stepney	Vstepney@central.uh.edu	UH Contracts Office
Jack Casey	jfcasey@uh.edu	UH EAS Department Chair
Laura Bell	lbell4@uh.edu	UH EAS Department Admin
June Zeng	jzeng2007@gmail.com	Team Member
Qiong Wu	qiongwu2010@gmail.com	Team Member
Johnny Seales	Johnny.seales@gmail.com	Team Member
Lee Bell	lee.bell@geokinetics.com	Geokinetics (Industrial partner)
Keith Matthews	kmatthews@fairfield.com	Fairfield (Industrial partner)
Subhashis Mallick	smallick@uwyo.edu	Univ. of Wyoming
Steve Stribling	SStribling@gmocks.com	Grand Mesa Production

CONTENTS

Executive Summary

This report presents major advances in progress made through the report period from January 1 to March 31 of 2011 for the CO_2 sequestration training project in the Dickman field, Ness County, Kansas (Figure 1).

The geology modeling work for the first quarter, 2011 focused on the evaluation of seal efficiency of the Middle to Upper Pennsylvanian carbonate and shale interbedded strata.

We investigated various strategies to estimate shear wave velocity to establish optimal elastic model for subsequent multi-component processing. The estimated shear wave velocity results show good consistency and low percentage in differences, indicating reliability of the shear wave profiles obtained.

We have done narrow band decomposition of 3D seismic data at the Dickman field using traditional band pass filters. Mid-frequency decomposition (41 Hz) indicates meander channel features without a broadband expression. Both potential fracture and channel features are being investigated using dense well control to confirm geological reality.

Geological modeling (June)

The geology modeling work for the first quarter, 2011 focused on the evaluation of seal efficiency of the Middle to Upper Pennsylvanian carbonate and shale interbedded strata. The CO2 injection model in 2010 predicted a high possibility of leaking from the 90-100 ft thick seals made of Middle Pennsylvania Fort Scott Limestone and the underlying clastic rocks on the Mississippian Unconformity. To further investigate the sealing efficiency in order to minimize leaking risks, the injection model is expanded to include the Upper Pennsylvanian strata.

The extended stratigraphic window for the seal evaluation in the Co2 injection model is shown by the blue rectangle in Figure 2, starting from the top of Upper Pennsylvanian Heebner Shale down to the Fort Scott Limestone top, totaling over 500 feet, with the Heebner Shale as the hanging datum. Four tops bounding the three major litho-zones were identified from most of the 32 wells with GR logs. From top down, they are Heebner Shale, Lansing Group, Marmaton Group, and the Pawnee limestone, as indicated by the the stratigraphic units in bolded letters of Figure 2.

A cross section (Figure 3) indicates the tops are laterally correlatable. In this section, both high GR and high Neutron porosity values are kicking to the right, therefore the shale-rich beds with low porosity are indicated by thin-waist-like shapes, compared with carbonate and sandstone layers. As shown by Figure 3, depths of some well tops (mainly carried from GeoFrame system) need further adjustments based on well log characteristics, especially for the Pawnee Limestone top, before being used as the stratigraphic unit boundaries for the model. The litho-zones bounded by them will be used as basic units for the stratigraphic, structure and property models. With plentiful well penetrations in the Upper Pennsylvanian strata for a reservoir-scale model, seismic data will be used mainly for structure and fracture analysis with the support from the regional geological deformation history.

For a better understanding of the deformation history, the shallowest regionally correlatable well top in both seismic and well data, Stone Corral, is shown by Figure 4. The depths of Stone Corral ranges 650 to 750 ft above sea level (or 1600-1700 ft MD). Since the tops are about 1600 ft above the hanging datum of the cross section in Figure 3, only the bottom part of this litho-zone is shown. The red beds made of sandstone and shale with thin-layer evaporates below the Stone Corral are unlikely to be good seals. However, the Stone Corral top map gives an overview of the structure framework with the simplest deformation history. It shows a northeast-plunging anticline with a steep NW flank bounded by the NE-trending fault (black dash line). This structural framework was finalized during the most recent structure episodes, probably as early as Late Cretaceous and as late as Eocene.

Figure 5 shows structure maps for Heebner and Lansing, and Figure 6 shows structure maps for the Marmaton Group and the Pawnee Limestone. The Upper Pennsylvanian tops in general show deformation by more structural episodes compared

with the Permian Stone Corral formation. However, some irregularities on maps are caused by the wrong picks of well tops carried from the Geoframe interpretations, after comparing each map with the ones above and below it. These errors are being corrected and resulted maps will be used to build the stratigraphic model, and to further subdivide zones of different lithology properties as the base for rock property calibration and gridding, such as rock porosity and interval velocity. The former can be used to generate a permeability grid input to the CO2 injection model, and the latter for the study of rock acoustic properties.

Shear wave velocity estimation (Qiong)

A major challenge to the project is lack of shear velocity logs in the survey area. We estimated shear wave velocity (Vs) from compressional wave velocity (Vp) by assigning the empirical Vp/Vs ratio to litho-zones interpreted from well logs. Vs results were generated by constraining input for strata composed of both carbonate and sandstone sections.

Elastic wave modeling typically employs Vp, Vs and density for the simulation of a full seismic wavefield. Well Humphrey 4-18 was chosen as study location for 1D elastic forward modeling since it has a full log suit for lithology study and a full penetration to the Osage CO_2 storage candidate (Figure 7). We observe that quality of density log and resistivity log of Humphrey 4-18 is not ideal, they are degraded by anomalous low and high values.

Lithology and fluid volume affect the S-wave velocity and consequently the Vp/Vs ratio, and there are many mixed layers as well as pure shale, sandstone, limestone and dolomite in the Dickman section, therefore, we want to use local discriminators to determine lithology to establish the elastic model. We took four logs (gamma ray (GR), density (RHOB), resistivity (RILD) and sonic (DT)) of Humphrey 4-18 into account (Figure 7) and extrapolate to the depth interval where not all logs are available.

The target strata in Dickman Field contains three sections in depth with different lithology, the Fort Scott and Viola formation, which are in depth around 500m and 1000m respectively, indicate the depth where the changes begin: from surface to the Fort Scott the strata are dominated by sandstone-shale (depth ranges around 0 to 500m), in this section Vs by various methods are in agreement (fFgure 8). The relative difference of prediction is less than 5% except a few less than 10%. In the lower section from Fort Scott to Viola, dominated by inter bedded shale and carbonate, Vs results gave diverse trends due to different sensitivity of lithology (Figure 9). In deep section beneath Viola (dominated by carbonate) Vs predicted by the empirical method was generally higher than other methods, indicating either those methods are inappropriate for carbonate section or local calibration may be necessary (figure 10).

Our preliminary results show a good agreement to the sandstone-shale dominated shallow section. Further analysis is in progress for other sections with different lithology.

To better monitor CO2 storage, we investigated various strategies to estimate shear wave velocity to establish optimal elastic model for subsequent multi-component processing. The estimated shear wave velocity results show good consistency and low percentage in differences, indicating reliability of the shear wave profiles obtained.

CO_2 Flow to seismic (Jintan)

As introduced in previous reports, Gassmann fluid substitution constitutes the main part of rock physics modeling. A 1D convolutional model is used here to compute normal-incidence reflection coefficients, which are convolved with a seismic wavelet (Ricker). The horizontal grid of the flow simulation model consists of 33 by 31 grid cells with a resolution of 500x500ft. The vertical section represents 32 simulation layers and each vertical grid cell has varied depth increment that corresponds to the geological settings due to an unconformity at about -1980 ft subsea. In the previous test phase the seismic data was generated on this very coarse simulation grid (500 x 500ft); in this report, the data has been interpolated into the field seismic data bin grid of 82.5 x 82.5 ft, and sorted into different inlines and crosslines with correct headers. The new seismic dataset consists of 194 (inline) x 122 (crossline) traces with 1s time window (dt =2ms) with origin is in the southwest corner at absolute coordinates (1 562 247, 690 023) feet coincident with the Dickman field 3D seismic data origin.

In the current simulations, CO_2 is injected for 50 years, then the injection well is shut in and flow modeling continues for 150 years. Seismic volumes have been generated every year for this 150-year time interval. Compared with the previous results, the seismic resolution has been greatly improved by using a Ricker wavelet (zero phase, dominant frequency of 35hz) with a narrower width to reduce ringing and side lobes.

Figure 11 illustrates the post-injection CO_2 saturation changes for 16 simulation layers in the first (2002) and last year (2155) respectively. The new seismic dataset inline 86 and crossline 98 have the most significant CO_2 saturation change for these two years and have been pulled out for comparison (red lines in Figure 12). Figure 13(b) shows the CO_2 saturation distribution from flow simulation output corresponding to seismic inline 86. It's clearly seen that the difference on seismic data (as shown in Figure 14) is mainly caused by this partial increase of CO_2 saturation, which leads to 4% decrease of impedance.

Although the vertical representation is different, this feature has been shown on the same horizontal locations, which will also have the similar affect on seismic in the crossline direction (Figure 15). Figure 13(b) also gives a plot of porosity distribution that corresponds to the same seismic inline 86. This may help explain the lateral inconsistency in the seismic, one of the reasons might be poor interpolation of sparse porosity values from well logs. These interpolation artifacts did not much affect the flow simulation results as evidenced by a good history match. But they will have a strong influence on seismic response, representing a challenge for simulating realistic seismic data from the flow grids. However, this comparison result still can help us detect pore fluid variation by

CO_2 injection that may represent the unconformity locations, and moving forward, it may help us to study the fluid flow paths at various times.

Future work will include comparison with field data as a preliminary test to evaluate its feasibility as a baseline survey for time-lapse monitoring purposes. Also, a more sophisticated seismic forward modeling method will be investigated and a smoother and better-defined porosity distribution may help improve the seismic data quality.

Ultra-narrow band filtering (Johnny)

A trapezoid filter in Seismic MicroTechnology (SMT) Kingdom 3D seismic interpretation software was used to create data centered on 41 Hz (Figure 16). Two SMT trapezoidal filters were tested. The first used corner frequencies of 39 / 40 / 42 / 43 Hz. We term this filter A. The second filter (B) has 40.8 / 40.9 / 41.1 / 41.2 Hz. Each filter was used to create an attribute volume.

Visual inspection of time slices from SMT filters A and B showed no discernable difference, nor did they show any clear difference from filter A implemented in SU (Figure 17). Analyzing a 41 Hz volume at the 848 ms time slice, we observe a dark channel-like feature extending from the main channel to the yellow arrow of Figure 16. Figures 16 and 17 show the new channel feature is robust with respect to filtering in either SU or SMT.

We studied detailed variation between the narrow band results of SMT filters A and B by subtracting the resulting data volumes (Figure 19). There are, indeed, slight differences between the outputs from the two SMT filters. The difference plot shows energy in horizontal bands representing acquisition footprint (receiver orientation), a large fault in the NW corner, a bright karst (sinkhole) feature near the center, and a network of curved lineations of unknown origin. In an absolute sense, the maximum amplitude difference is on the order of 10% in the mentioned features, otherwise less that 2%.

We have done narrow band decomposition of 3D seismic data at the Dickman field using traditional band pass filters. Mid-frequency decomposition (41 Hz) indicates meander channel features without a broadband expression. Both potential fracture and channel features are being investigated using dense well control to confirm geological reality.

Mapping deep structure (Shannon)

This section reports results of using 3D seismic data and sparse well control from the Dickman field to map pre-Pennsylvanian formations in the Dickman Field area. We focus on formations in the lower Mississippian (Osage and Gilmore City) and in the Ordovician (Viola). The primary storage candidate in the Dickman field is a deep saline aquifer located in the Osage formation. Deep saline aquifers are excellent potential CO2 storage candidates, but significant pre-storage characterization is required to determine suitability.

The main objective is to investigate possible CO_2 migration pathways. Both time and depth structure maps of the Osage, Gilmore City and Viola formations were produced and interpreted. Several seismic attributes were interpreted to highlight small faults and fractures. Seismic attributes such as coherence, curvature, SPICE, and ANT play a vital role in this study.

The focus of this study is to map deep structure in Ness County, Kansas and determine if a deep saline aquifer has the potential to be a CO_2 storage candidate. The Dickman field in Ness County, Kansas is approximately 3.325 square miles (Figure 1) and has a production history of about 1.7 million barrel of oil dating back to its discovery in 1962. Our work uses SMT KINGDOM software for 3D and seismic interpretation to map structure of deep formations in the lower Mississippian and Ordovician.

The storage target being investigated in this study is a porous saline aquifer in the Mississippian Osage formation. This aquifer is a primary sequestration target and the upper Mississippian oil reservoir is a secondary storage target. The oil/water contact is at approximately 1981 feet subsea and there is an oil column of about 35 feet. Between the Mississippian and the overlying Pennsylvanian shale and conglomerates of the Cherokee Group there is a karsted regional unconformity contact. Sandstones from the Lower Cherokee group that are locally deposited on the sub aerial karst and form a second oil reservoir (Liner et. al., 2010).

In 2001 a 3D seismic survey, approximately 3.325 square miles, was conducted in the Dickman Field. Survey acquisition parameters are shown in Table 1.

Original data processing was by Sterling Seismic Services, but we worked with a prestack time migration volume generated at the U of Houston Allied Geophysical Lab. Dominant frequency in the data is about 32.5 hertz, giving vertical resolution ($\lambda/4$) in our area of interest as 122 ft. (37.2 m) and lateral resolution ($\lambda/2$) of 244 ft. (74.4 m). There are 142 wells in the Dickman Field but only four penetrate the deep horizons of this study (Figure 20). The Humprey 4-18, Stiawalt 3 and Sidebottom 6 wells have formation tops for the Osage, Gilmore City and Viola formations. The Schaben 4 well only penetrates the Osage and Gilmore City formations.

Well	**Formation**	**Top (SS ft)**
1. Humphrey 4-18	Viola	-2163
2. Schaben 4	Gilmore City	-2135
3. Stiawalt 3	Viola	-2260
4. Sidebottom 6	Viola	-2239

Investigation of the deep saline aquifer is primarily seismic due to sparse well control in the pre-Miss. section. The purpose of this investigation is to use seismic attributes to map fractures and yield contributing evidence that the deep saline aquifer can be an adequate storage candidate for CO_2. Seismically mappable fractures beneath the Mississippian unconformity have previously been reported (Nissen et al., 2009).

Figure 21 shows our deep structure mapping workflow for the Dickman Field. Formation tops were first tied to the 3D seismic volume by creating synthetic seismograms using the two wells that have sonic and density logs (Humphrey 4-18 and Sidebottom 6). This establishes the time/depth (T-D) relationship of the Osage, Gilmore City and Viola formations in the seismic, which then allows horizon picking throughout the volume. After finalizing the synthetics, Osage, Gilmore City and Viola horizons were tracked on amplitude throughout the 3D image area to create time horizons and grids. Depth structure maps were generated using the Elmore 3 T-D curve.

Small faults and fractures were picked throughout the seismic volume first on amplitude data, then SPICE (Smythe et al., 2004) for better visualization of discontinuities. Additional attributes were then used for surface mapping and interpretation of faults and fractures in order to classify discontinuity picks as probable, possible or doubtful. Isopach maps were created as a final step in the interpretation process.

Only two out of the four deep wells were viable for synthetic seismogram generation, specifically Sidebottom 6 and Humphrey 4-18. Synthetic seismograms were created for each of these wells, but there were problems: (1) The Humphrey 4-18 is on the edge of the 3D seismic area, (2) The Sidebottom 6 is ~750 ft. (229 m) outside the 3D seismic area, (3) Both synthetics had a correlation coefficient well below 0.1, (4) Humphrey 4-18 has questionable density and sonic logs

To address problems 1 and 2, the Humphrey 4-18 and Sidebottom 6 were ‘moved’ about 0.5 mile inside the 3D seismic area by creating dummy, or mock, wells (DH-4-18 and DS6), see Figure 22.

This is justified since most horizons in Dickman are laterally continuous (layer cake geology). The better of the two synthetic seismograms was chosen to tie the geology to our seismic data at the Dickman field.

Using 3D seismic data and attributes, we observe a prominent channel at the Miss./Penn. unconformity surface with an imprint of the channel vaguely observed in the time structure of Viola and increasingly prominant as we move up to the Gilmore City and then Osage. The meander portion of the channel is also evident in the Osage amplitude map (figure 23).

In addition, a velocity sag theory was tested in order to confirm that the channel imprint is indeed true geology and not a result of sag. We conclude the karst topography present at the Miss./Penn boundary must extend all the way down to the Viola.

Well logs assisted with the interpretation of amplitude maps. Random amplitude clusters are likely representative of karst areas. Well logs confirm the presence of dolomite and other carbonate minerals that may contribute to the polarity of each amplitude map. Many of the amplitude anomalies, especially at the Osage level, follow the trend of the Miss./Penn. channel imprint.

Interpretation of the attribute maps, along with observing and picking discontinuities in both amplitude and SPICE, aided in the verification of faults/fractures and their classification. Each attribute has a different value in highlighting these discontinuities. For instance, SPICE attribute was helpful for fault/fracture identification in vertical section rather than map view. Only amplitude and SPICE could be analyzed in vertical section. Variance seemed to display a better correlation with discontinuity picks and produced better visualization than coherence (figure 24). Variance also highlighted the Miss./Penn. channel well and was used as preprocessing for the ANT process.

Curvature maps produced more anomalous areas than most of the other attributes and ANT tracking (from variance) generated the most accurate correspondence with the fault/fracture picks. All of the fault/fracture picks corresponded to ANT features and some continued a little further in areas where the discontinuity picks stopped. However, there are many ANT features that have no expression in other attributes, despite double-checking to confirm this statement.

Table 2 shows fault/fracture classification characteristics. Each feature is checked if it had extent, was observable on a particular attribute and was not affected by noise or edge effects. Discontinuities are classified (Table 3) as probable if they have significant extent and were seen on all attributes analyzed. Features 7, 10 and 13 were considered probable faults. Some of these were near the edge of the survey, including the main fault, but none were likely to be an artifact or noise.

Only two fault/fracture picks (6 and 12) were placed into the “possible” category. Discontinuity pick 6 was seen on all attributes and was not near the edge of the survey, but it did not have extent. Pick 12 had extent, corresponded with four out of five of the analyzed attributes but it was located near the edge of the survey and looked as though it could be due to edge effects. The remaining fault/fracture picks did not have extent, corresponded with four or less attributes and were either noise induced, had edge effects, or both.

Figure 25 shows all fault/fracture picks that were made, and Figure 26 shows the probable fault/fracture picks on the Osage ANT attribute. Note the large number of ANT features that are not observed consistently in other attributes.

Carbon Capture and Storage (CCS) is a developing technology that requires detailed subsurface characterization. The Dickman field serves as a pilot project for CCS with a porous saline aquifer at the Osage formation. Deep formations were mapped in the Dickman field to evaluate structure, faults, and possible fractures. The methods for this investigation included use of several seismic attributes to detect small faults or fractures. It is important to know the validity and location of these features as they could serve as possible CO_2 leakage pathways.

Amplitude and SPICE data were both carefully examined in vertical section to pick discontinuities and several different attributes were investigated to confirm these features. Allowing for data quality, there are 4 out of the 20 discontinuity picks considered to be

probable small faults or fractures; 3 of the 4 trend northeast-southwest in agreement with the orientations reported by Nissen et al. (2009).

Work Plan for the next quarter

Elastic modeling: By next quarter we will still utilize forward modeling to test the effect of density, to see if we could avoid inputting density log which is in poor quality in S wave velocity estimation for Humphery 4-18, and obtain synthetic elastic seismic data based on the optimal elastic model that was built.

Flow to seismic: comparison with field data as a preliminary test to evaluate its feasibility as a baseline survey for time-lapse monitoring purposes. Also, a more sophisticated seismic forward modeling method will be investigated and a smoother and better-defined porosity distribution may help improve the seismic data quality.

Ultra narrow band filtering: We plan to refine the use of filters to better isolate single frequencies. To validate the channel indicators in NB data, we will compare well log data in and out of the features looking for structural, lithologic, rock property, or stratigraphic changes that may account for the observed features. Once formation tops and sequences have been established, the logs can then be utilized to build a geologic cross section of the area. This will allow structural and stratigraphic interpretation. Once this has been completed, it will be possible to tie this information to the seismic volume. The seismic volume itself will also be interpreted to determine if there are any visible signs of the channel extension. Both potential fracture and channel features are being investigated using dense well control to confirm geological reality.

Cost and milestone status

Baseline Costs Compared to Actual Incurred Costs…. Needs update

1/1/10 – 3/31/10	Plan	Costs	Difference
Federal	$36,668	$23,415	$3,253
Non-Federal	$4,063	$0	$4,063
Total	$40,730	$23,415	$17,316

Forecasted cash needs Vs. actual incurred costs

Notes:
(1) Federal plan amount based on award of $293,342 averaged over 8 reporting quarters.
(2) Non-Federal plan amount based on cost share of $32,500 averaged as above.
(3) Cost this period reflects salary for J. Zeng (3 mo), Q. Wu (3 mo), J. Seales (3 mo).

Actual Progress Compared to Milestones

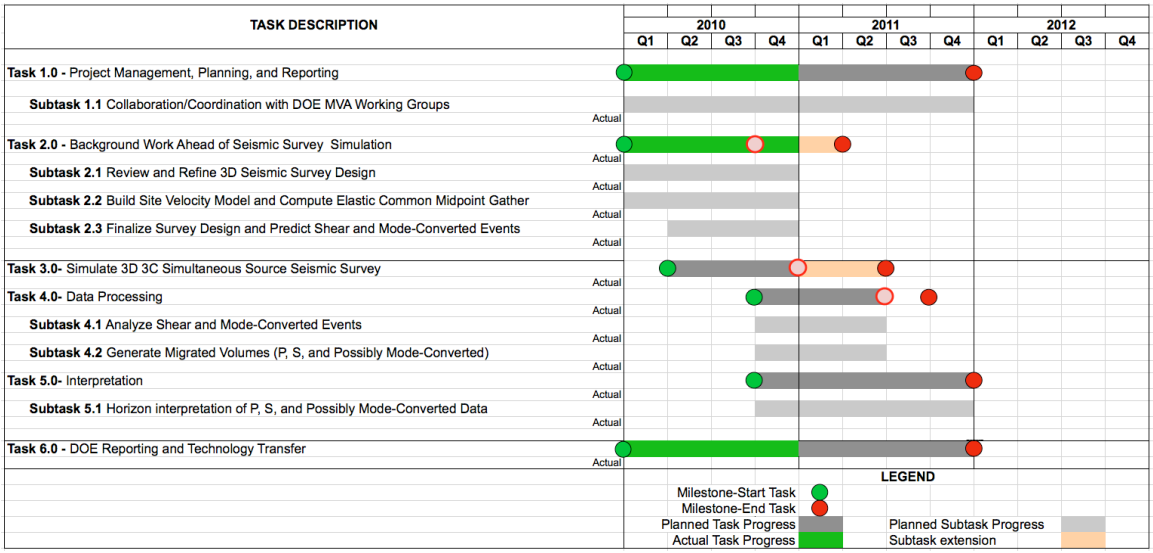

Personnel

Prof. Christopher Liner is Principle Investigator and lead geophysicist. He is a member of the SEG CO_2 Committee, Associate Director of the Allied Geophysical Lab, and has been selected to deliver the 2012 SEG Distinguished Instructor Short Course.

Dr. Jianjun (June) Zeng has been working exclusively on this project since Dec 2007 and is lead geologist.

Shannon Leblanc has completed and defended her Geophysics MS degree and is joining Marathon Oil Company as a geophysicist.

Ms. Qiong Wu is a graduate PHD student in geophysics who joined the project in January 2010 as a research assistant. She will be funded year-round out of the project.

Mr. Johnny Seales is an undergraduate student majoring in Geology and Geophysics. He is also a U.S. Army veteran, having served in Iraq. He will be funded year-round from the project. He anticipates earning his undergraduate degree in Dec. 2011.

Ms. Jintan Li is a 2nd year PhD student in geophysics who joined the project in Aug 2009. She is funded by Allied Geophysical lab at this time. Her thesis will be time-lapse seismic modeling (4D) for conducting dynamic reservoir characterization of the Dickman Field.

Tim Brown is a graduate MS student working on low frequency fracture indicators.

Bryan Flynn is a graduate student in the Professional MS degree program working on discontinuity mapping with attributes at the Miss-Penn unconformity

Eric Swanson is a part-time graduate MS student working on amplitude interpretation at the Miss-Penn unconformity. He is a full time employee of Swift Energy.

Technology transfer activities

3D Geologic modeling toward a site-specific CO2 injection simulation
Jianjun Zeng, Christopher Liner, Po Geng and Heather King
Presented at AAPG 2011

A CO_2 Sequestration Simulation Case Study at the Dickman Field, Ness Co., Kansas
Christopher Liner, Po Geng, Jianjun Zeng, Heather King and Jintan Li
Accepted for SPE 2011

Comparison on shear wave velocity estimation in Dickman field, Ness County, Kansas
Qiong Wu*, and Christopher Liner
Submitted to SEG 2011

A Time-Lapse Seismic Modeling Study for CO_2 Sequestration at the Dickman Oilfield, Ness County, Kansas
Jintan Li, Christopher Liner, and Po Geng
Submitted to SEG 2011

Channel and fracture indicators from narrow-band decomposition at Dickman field, Kansas
Johnny Seales, Tim Brown and Christopher Liner
Submitted to SEG 2011

Contributors

Christopher Liner (P.I, Geophysics)
Jianjun (June) Zeng (Geology and Petrel Modeling)
Qiong Wu (Geophysics PhD candidate)
Johnny Seales (Geology and Geophysics Undergraduate)
Jintan Li (Geophysics PhD candidate)
Shannon Leblanc (Geophysics MS)

References

Blumentritt, C.H., Marfurt, K.J. and Sullivan, C.E., 2006, Volume-based Curvature Computations Illuminate Fracture Orientations – Early to Mid-Paleozoic, Central Basin Platform, West Texas: Geophysics, Vol. 71, NO. 5, B159-166

Brown, A.R., 2001, Understanding Seismic Attributes: Geophysics, Vol. 66, NO. 1, 47-48

Castagna, J., 2011, Personal Communication: Direct Hydrocarbon Indicators Class

Chopra, S. and Marfurt, K., 2007, Seismic Attributes for Prospect Identification and Reservoir Characterization: SEG Geophysical Developments Series No. 11

Chopra, S. and Marfurt, K., 2008, Seismic Attributes for Stratigraphic Feature Characterization: Back to Exploration-CSPG CSEG CWLS Convention

Fang, Y., Baojun, B., Dazhen, T., Dunn-Norman, S. and Wronkiewcz, D., 2010, Characteristics of CO_2 Sequestration in saline aquifers: Pet. Sci. 7:83-92

Jewett, J.M., Bayne, C.K., Goebel, E.D., O'Connor, H.G., Swineford, A. and Zeller, D.E., 1968, The Stratigraphic Succession in Kansas: Kansas Geological Survey Bulletin, 189

Liner, C., Zeng, J., Geng, P., King, H., Li, J., Califf, J. and Seales, J., 2010, 3D Seismic Attributes and CO_2 Sequestration: DOE Final Report

Liner, C., Li, C.F., Gersztenkorn, A., and Smythe, J., 2004, SPICE: A New General Seismic Attribute: SEG Int'l Exposition and 74th Annual Meeting

National Energy Technology Laboratory, 2010, Best Practices for: Geologic Storage Formation Classification: Understanding Its Importance and Impacts on CCS Opportunities in the United States, DOE/NETL-2010/1420

Nissen, S.E., Carr, T.R., Marfurt, K.J., and Sullivan, E.C., 2009, Using 3-D seismic volumetric curvature attributes to identify fracture trends in a depleted Mississippian carbonate reservoir: Implications for assessing candidates for CO_2 sequestration: AAPG Studies in Geology 59, 297-319

Plasynski, S, D. Deel, L. Miller, and B. Kane, 2007, Carbon sequestration technology roadmap and program plan: U.S. Department of Energy, Office of Fossil Energy, National Energy Technology Laborator, e-report

Sawyers, C. and Wilson, T., 2010, An Introduction to this Special Section: CO_2 Sequestration: The Leading Edge, Vol. 29, No. 2, p. 148-149

Sheriff, R. E., 1991, Encyclopedic Dictionary of Applied Geophysics, third edition.

Smythe, J. and Gersztenkorn, A., 2004, Gulf of Mexico shelf framework interpretation using a bed-form attribute from spectral imaging: The Leading Edge, Vol. 23, No. 9, p. 921-926

Tables

Source	Vibroseis
Sweep	20-128 Hz, 12 s
Shot interval	165 ft, 45 deg NW-SE
Shot line interval	880 ft
Receiver interval	220 ft
Receiver line interval	660 ft
Time sample rate	2 ms
Interpolated bin size	82.5 x 82.5 ft
Inlines, Crosslines	158, 169

Table 1. Dickman 3D seismic survey acquisition parameters.

Feature #	Extent	Amplitude vertical section	SPICE vertical section	ANT	Coherence/ Variance	Curvature	Noise Induced	Edge Effects
Main-1	√	√	√	√	√	√		√
2*		√	√		√		√	√
3*		√	√		√		√	
4*		√	√	√		√		√
5*			√	√	√	√	√	
6		√	√	√	√	√		
7	√	√	√	√	√	√		√
8		√	√	√	√		√	√
9			√		√		√	
10	√	√	√	√	√	√		√
11		√	√	√	√			√
12	√	√	√	√	√			√
13	√	√	√	√	√	√		√
14		√	√		√	√		√
15*			√	√	√	√		
16		√	√	√	√	√	√	√
17*			√	√	√	√		
18*						√		
19*		√	√		√	√		
20*		√	√	√	√			√

Table 2 Discontinuity classification results. Asterisk denotes features not displayed on horizons but seen in time-slice and/or VuPack.

Probable	Possible	Doubtful
Main-1	Feature 6	Feature 4
Feature 7	Feature 12	Feature 5
Feature 10		Feature 8
Feature 13		Feature 9
		Feature 15
		Feature 16
		Feature 17
		Feature 18
		Feature 19
		Feature 20

Table 3. Summary table identifying mapped features.

Figures

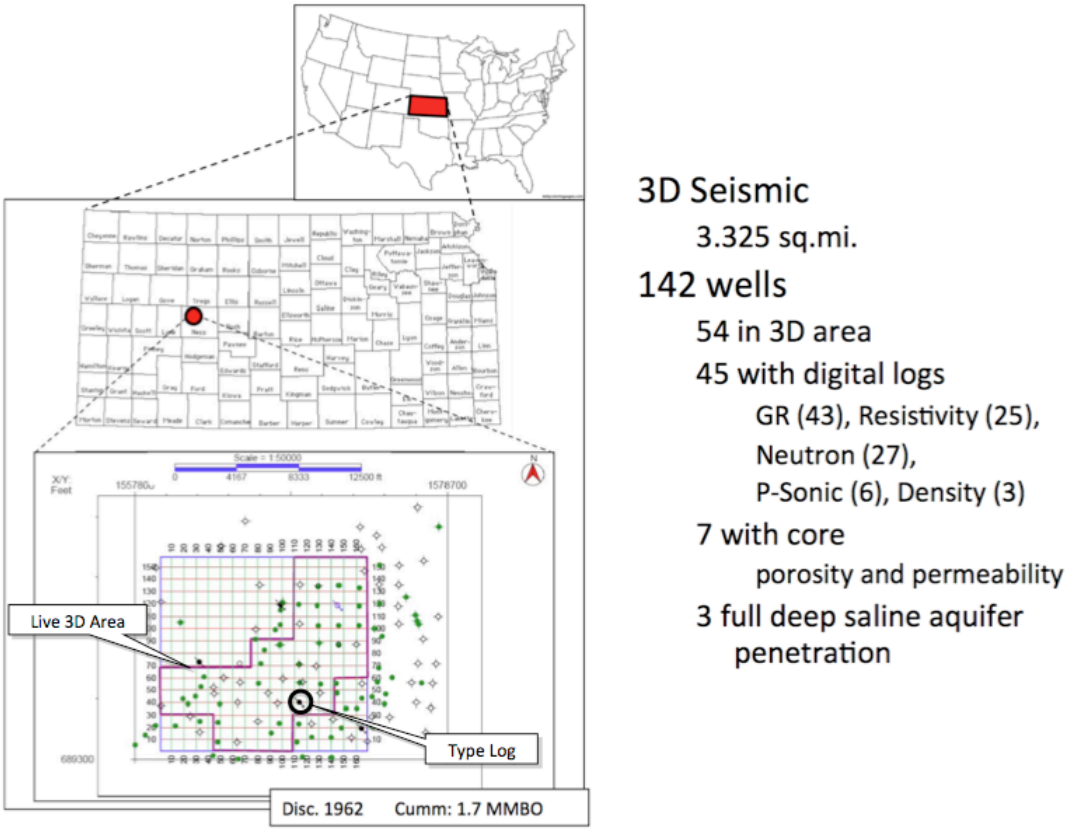

Figure 1. Dickman field site and description of available data.

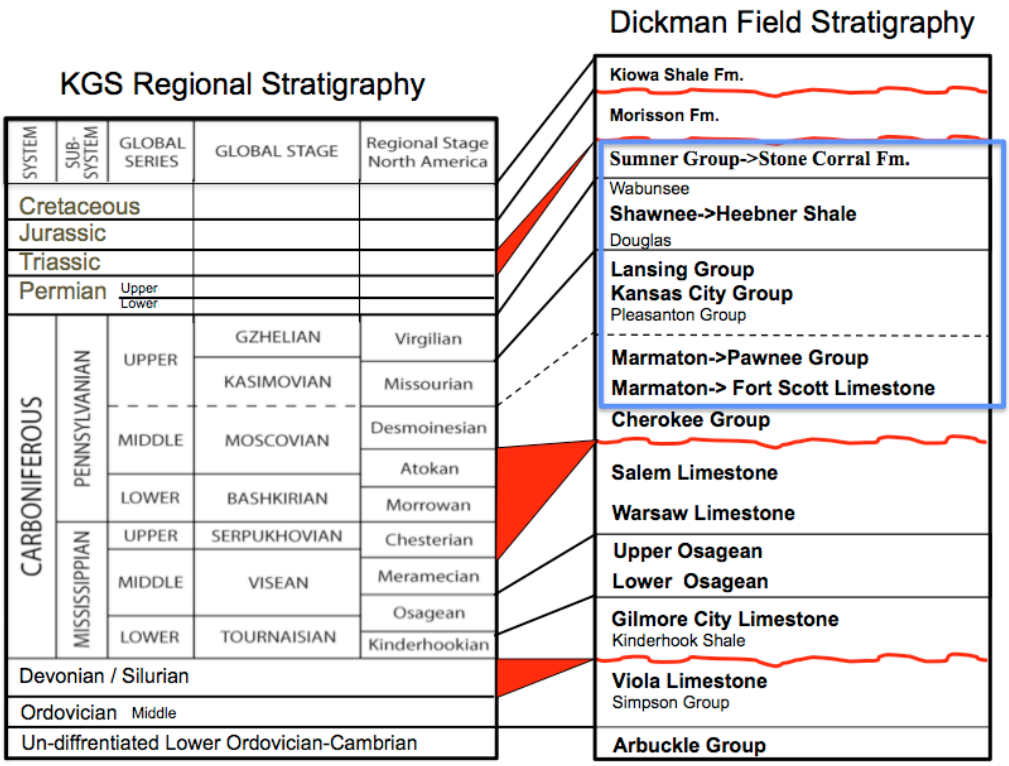

Figure 2. Chart to the left is the stratigraphic rank accepted by the Kansas Geological Survey (Sawin et al., 2008). The chart to the right shows correlation to Dickman local stratigraphic units, with higher confidence correlations in bold. Blue box indicates stratigraphy added to flow simulation model in this quarter.

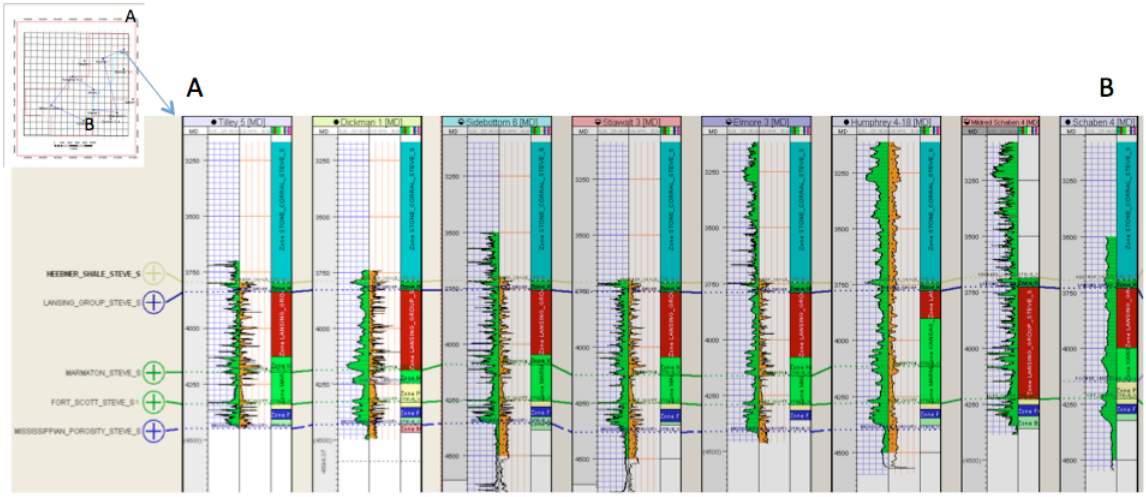

Figure 3. Cross-well correlation of selected tops and litho-zones bounded by these tops for the shallow seal interval. The hanging datum is 3100 ft MD. The GR log Porosity log are plotted in green and brown, respectively.

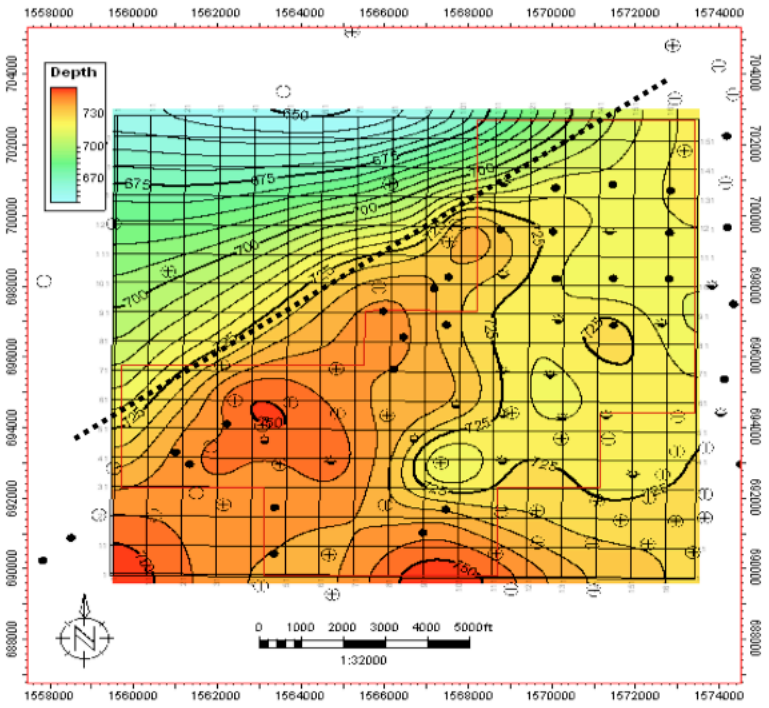

Figure 4. Stone Corral depth map, 650 -750 ft above sea level . The black dash line indicates the NE fault cutting on the NW flank of the anticline. The map was based on geological tops in over 70 wells, carried from the interpretation on GeoFrame system, or obtained from the Kansan Geological Survey Database and validated by at least 10 well logs.

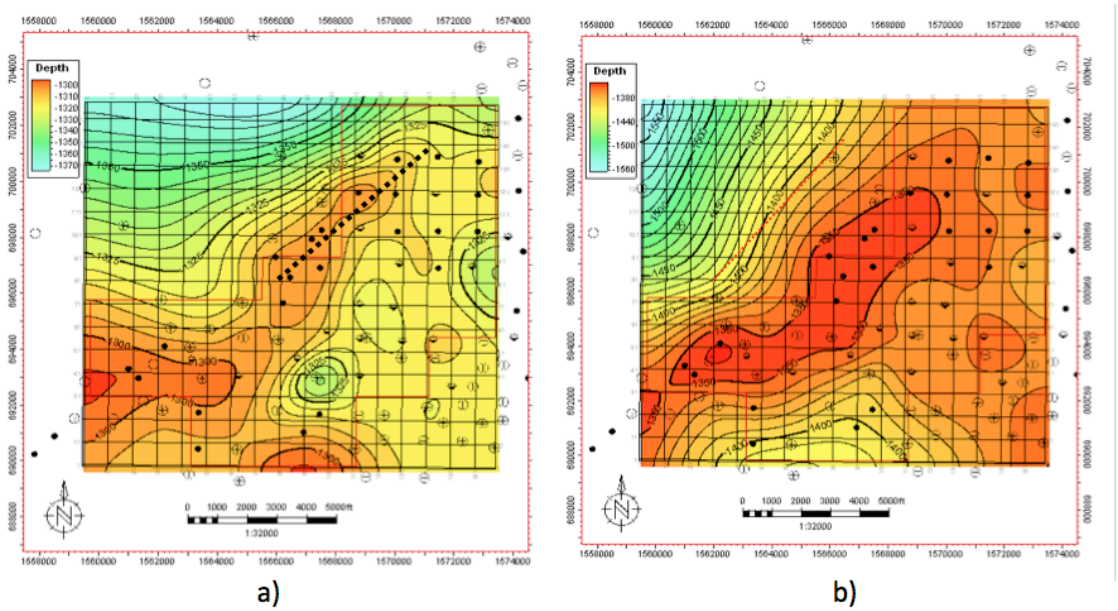

Figure 5: Structure maps for the shallower tops: (a) Heebner Shale, (b) Lansing Group. The Upper Pennsylvanian strata shows deformation by more structure episodes compared with the Permian Stone Corral Formation.

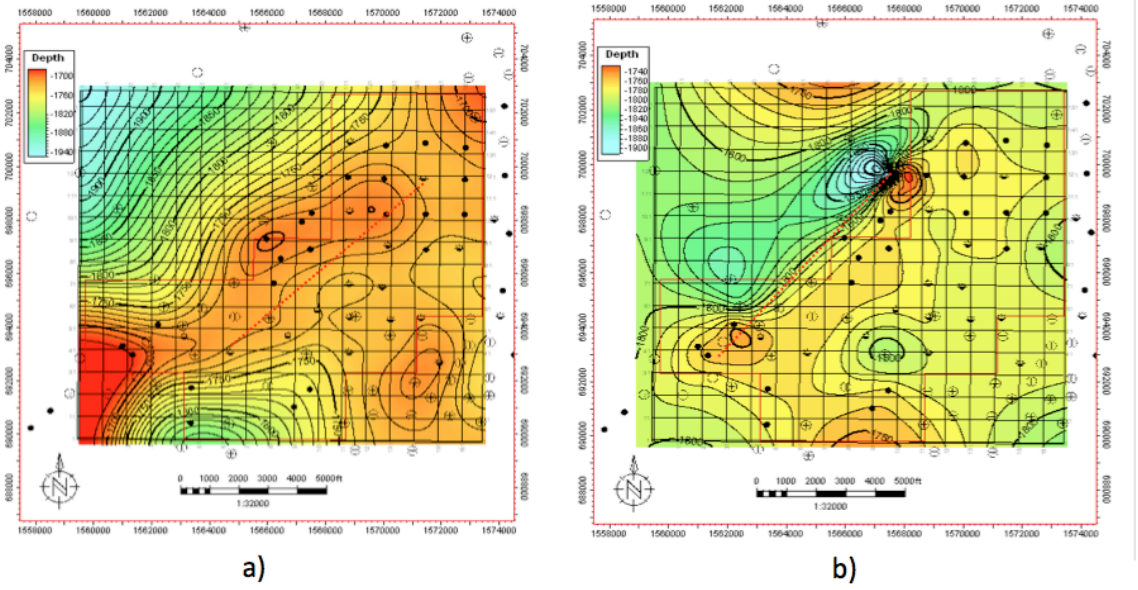

Figure 6: Structure maps for the shallower tops (a) Marmaton Group, (b) Pawnee Limestone. The Upper Pennsylvanian tops shows deformation by more structure episodes compared with the Permian Stone Corral Formation.

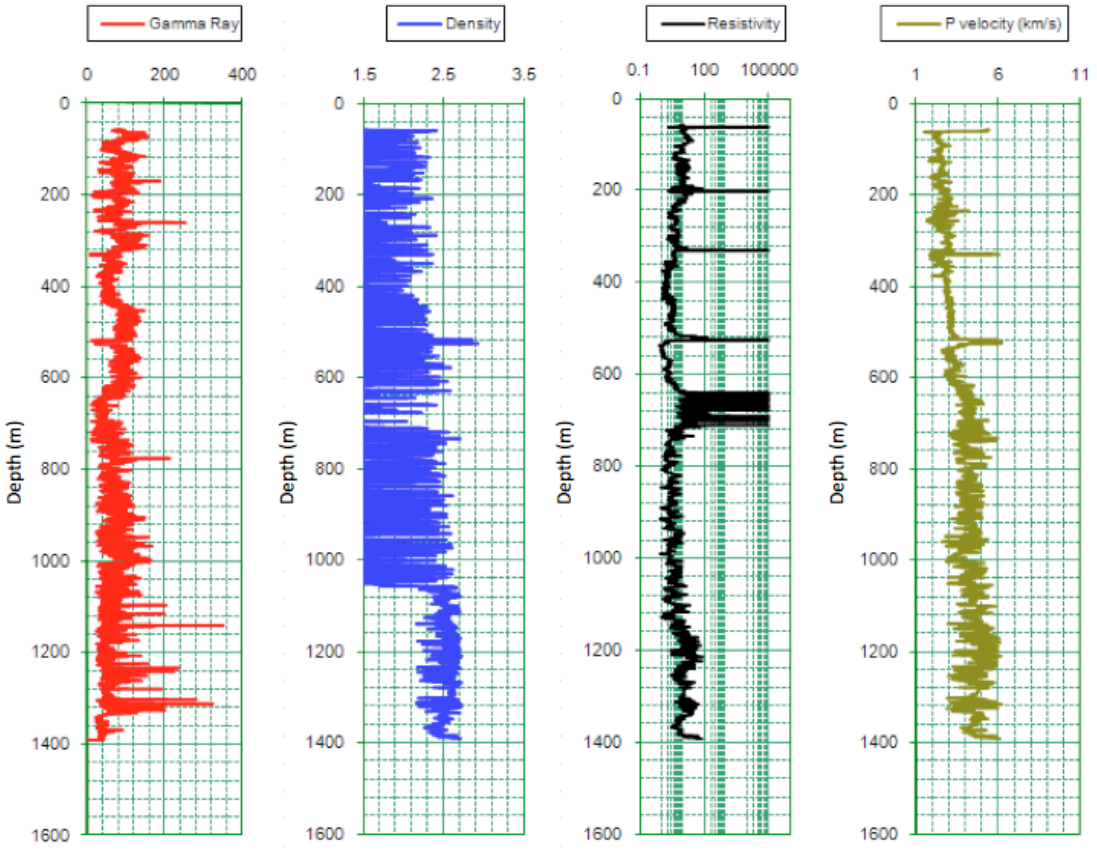

Figure 7. Humphery 4-18 input logs (left-to-right: gamma ray, density, resistivity and sonic log). Density in g/cc and resistivity in ohm-m.

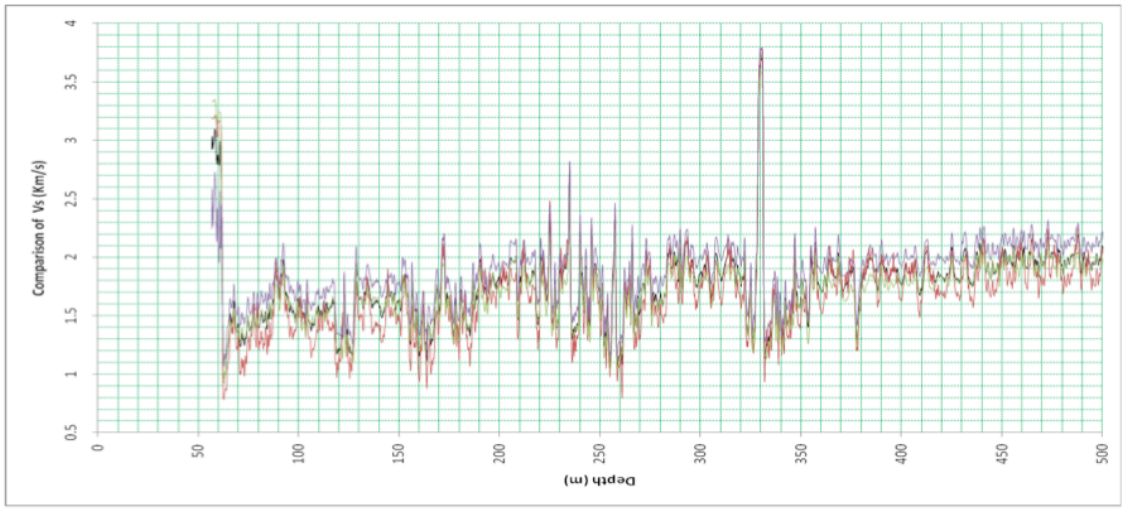

Figure 8. Comparison of Estimated Vs in depth between 0 - 500m by geology constrain method (black), empirical method (red), Gassmann method (green), and Xu-white method (purple).

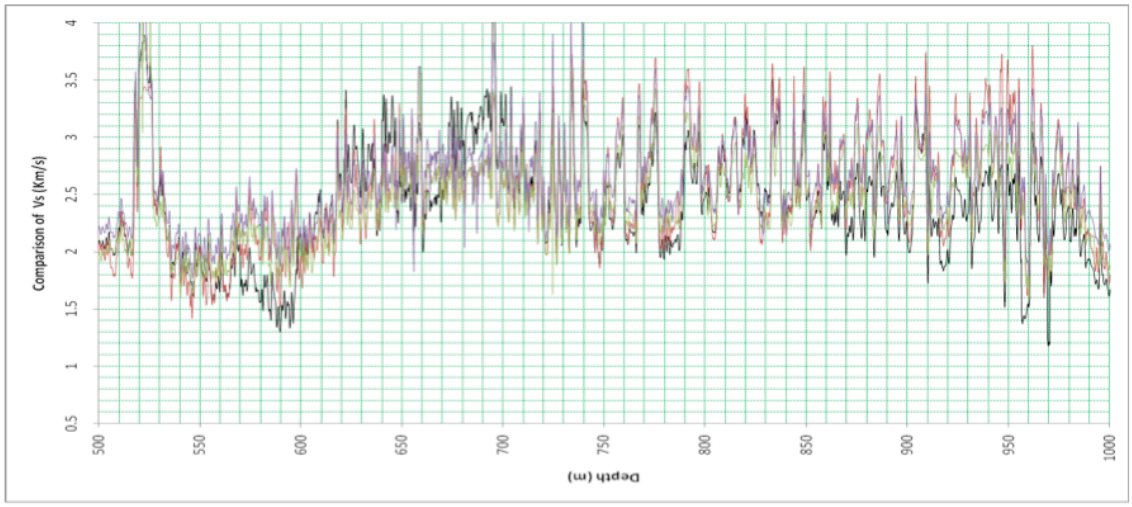

Figure 9. Comparison of Estimated Vs in depth between 500 -1000 m by geology constrained method (black), empirical method (red), Gassmann method (green), and Xu-white method (purple).

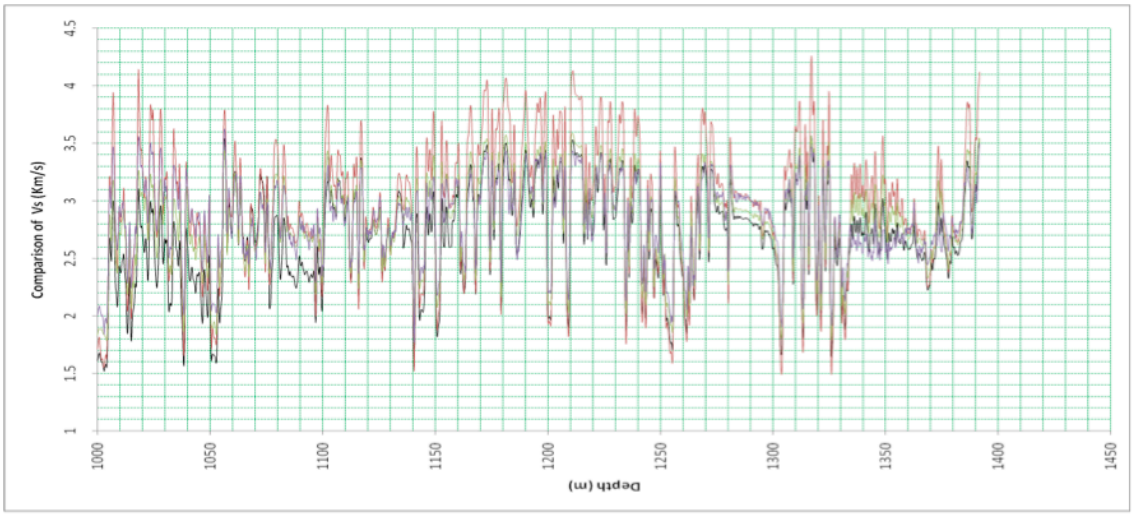

Figure 10. Comparison of Estimated Vs in depth between 1000 -1450 m by geology constrain method (black), empirical method (red), Gassmann method (green), and Xu-white method (purple).

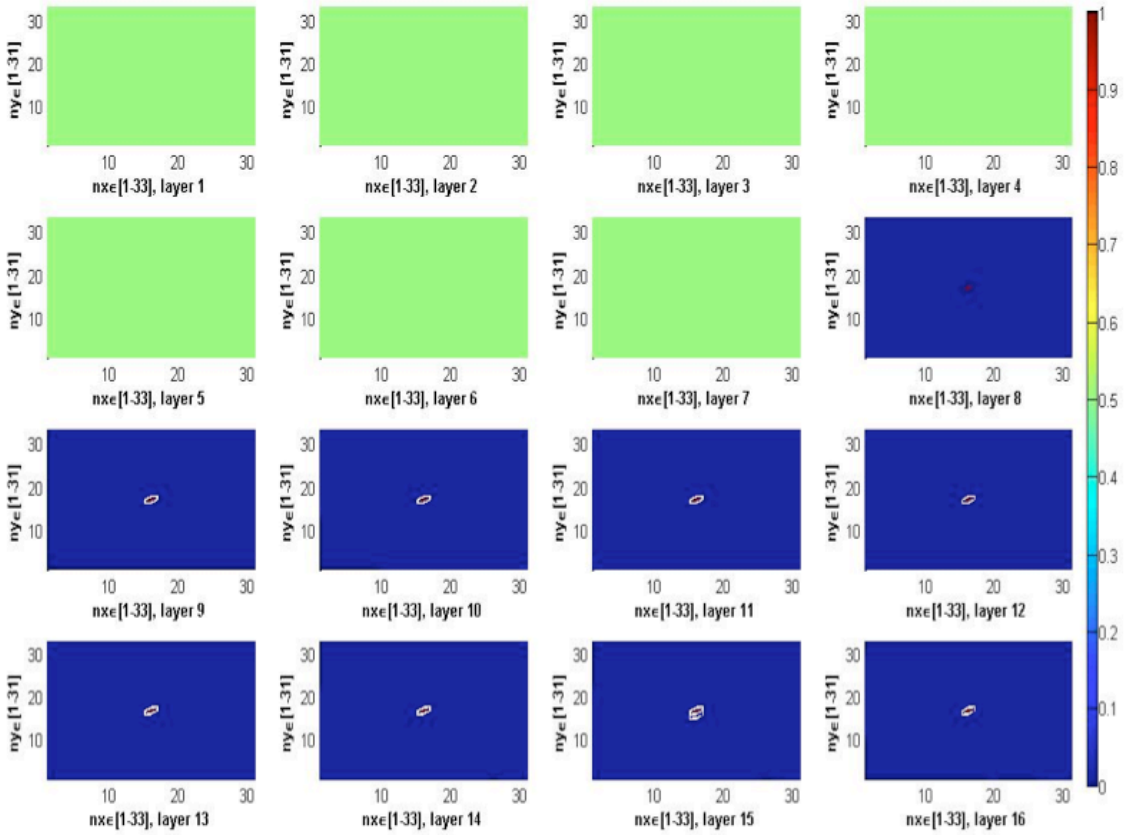

Figure 11. CO2 saturation for simulation layers from 1 through 16 for years 2002.

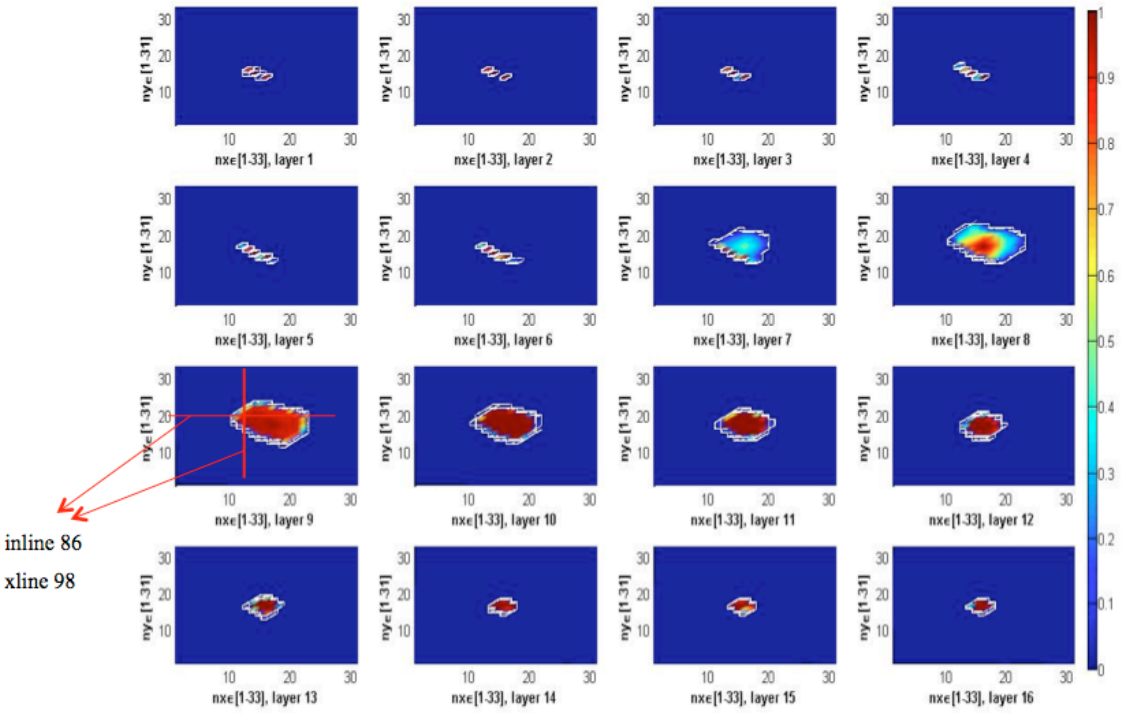

Figure 12. CO2 saturation for simulation layers from 1 through 16 for years 2155. Two seismic lines (inline 86 and crossline 98) are highlighed in layer 8 for comparison.

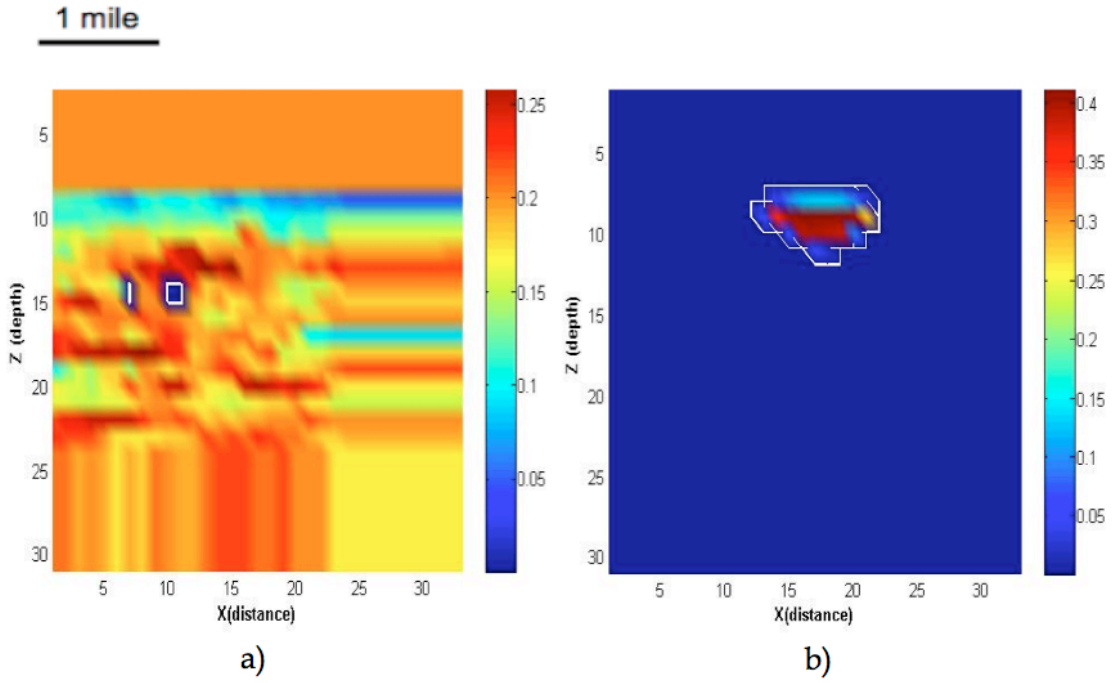

Figure 13. Vertical sections related to inline 86 for year 2155. (a) Porosity distribution. (b) CO2 saturation.

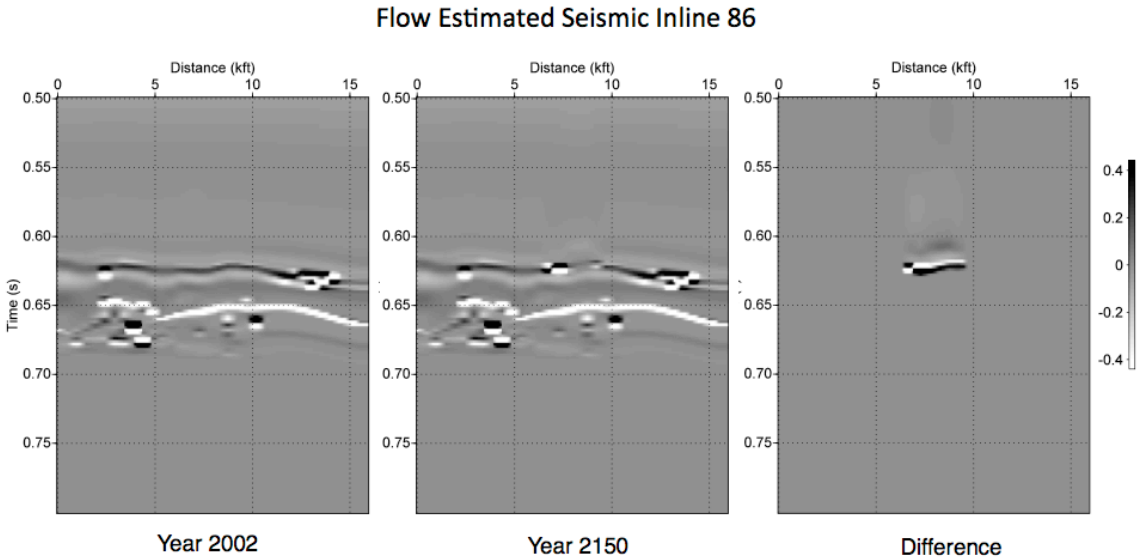

Figure 14. Estimated seismic inline 86 at the different simulation years 2002, 2150, and the difference. Data displayed from 500 to 800 ms.

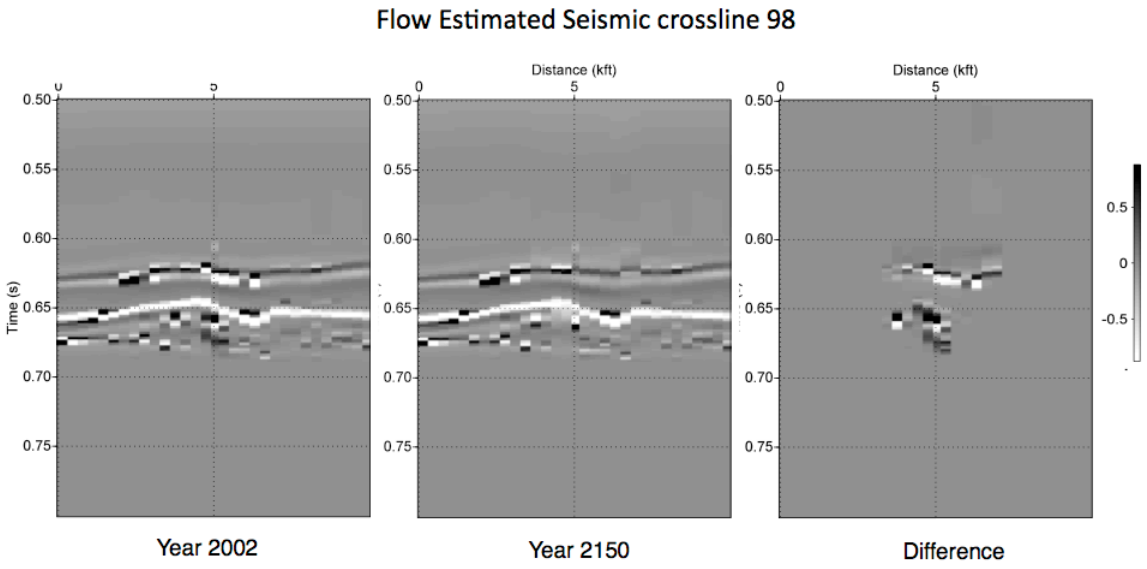

Figure 15. Estimated seismic crossline 98 at the different simulation years 2002, 2150, and the difference. Data displayed from 500 to 800 ms.

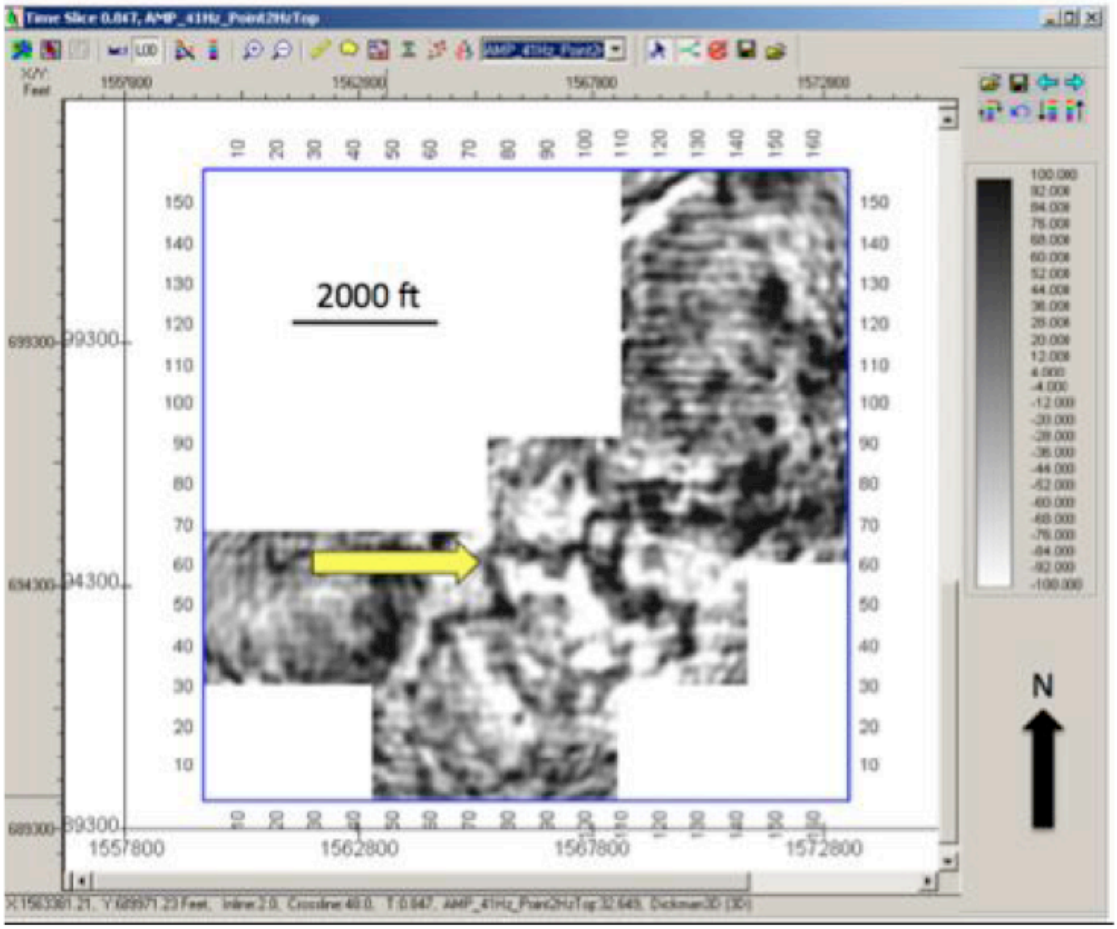

Figure 16. Narrow band time slice (847 ms) created with SMT filter B (0.2 Hz top). Yellow arrow indicates a possible channel feature not seen in broadband data.

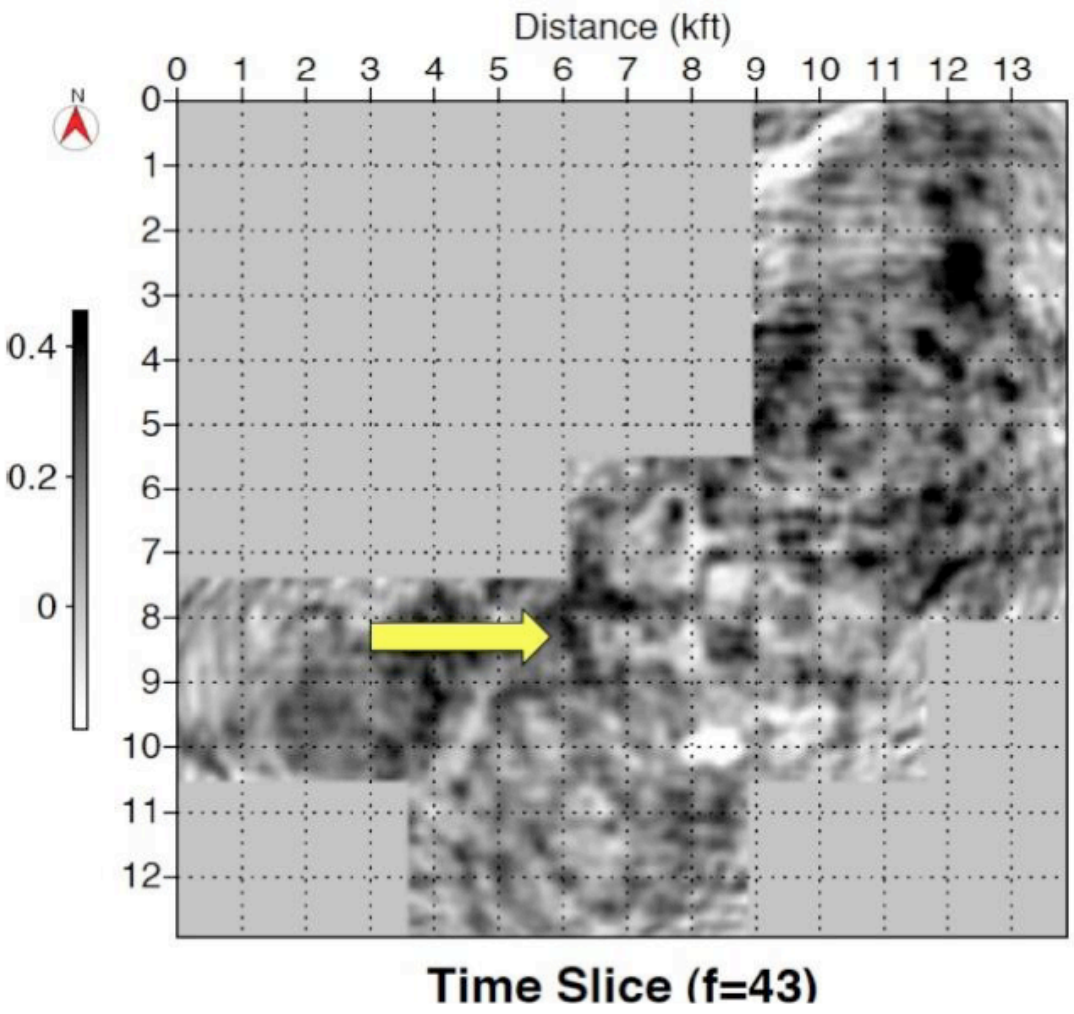

Figure 17. Seismic unix narrow band (43 Hz) time slice at 848 ms. Yellow arrow indicates possible channel feature not seen in broadband data (Figure 18).

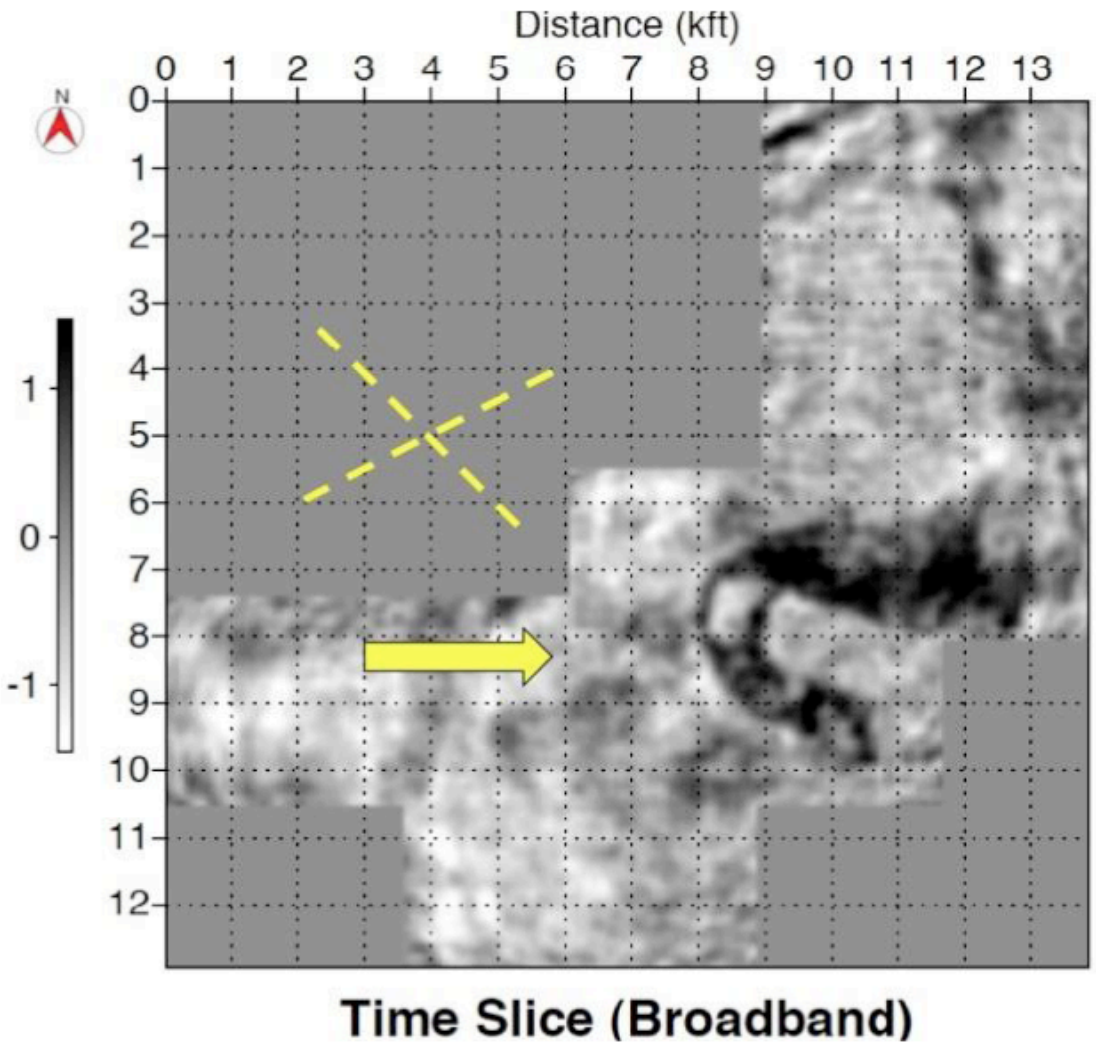

Figure 18. Broadband time slice at 848 ms, approximately coincident with the Miss/Penn unconformity. Features observed in narrow band data (Figure 16 and 17), but not on the broadband data, are indicated in yellow.

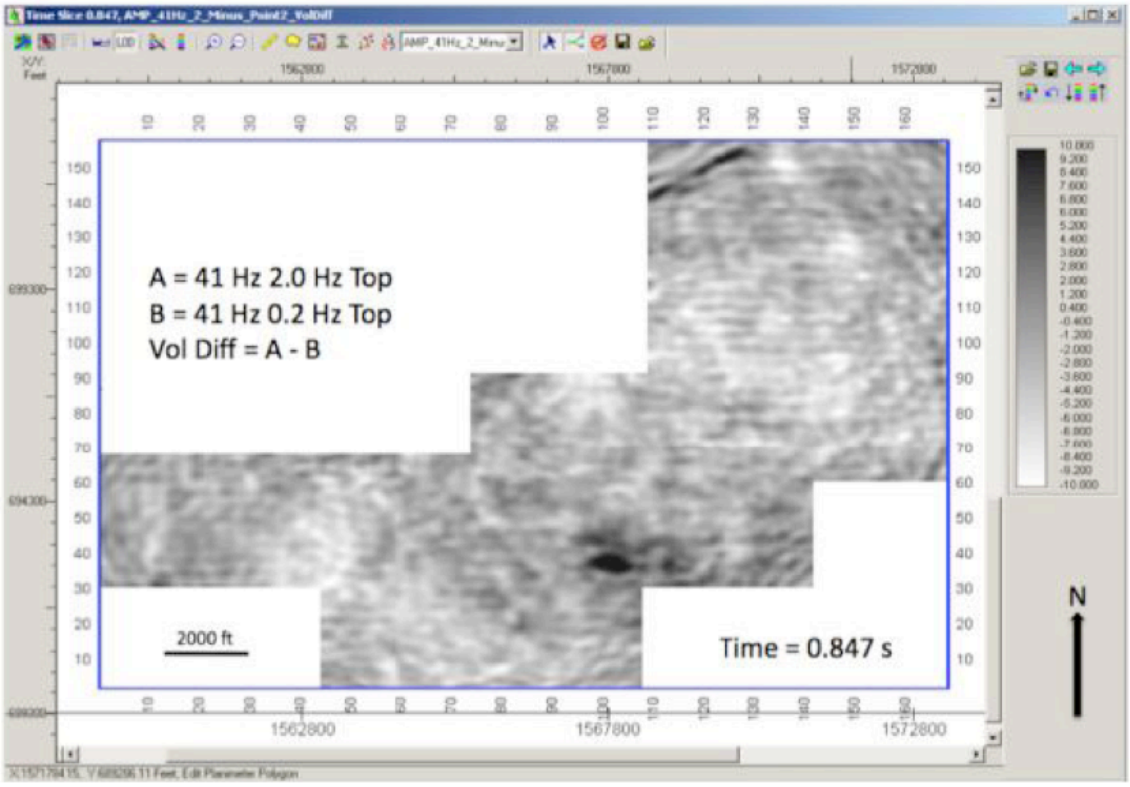

Figure 19. Time slice (847 ms) through difference volume created by subtracting SMT filter volumes.

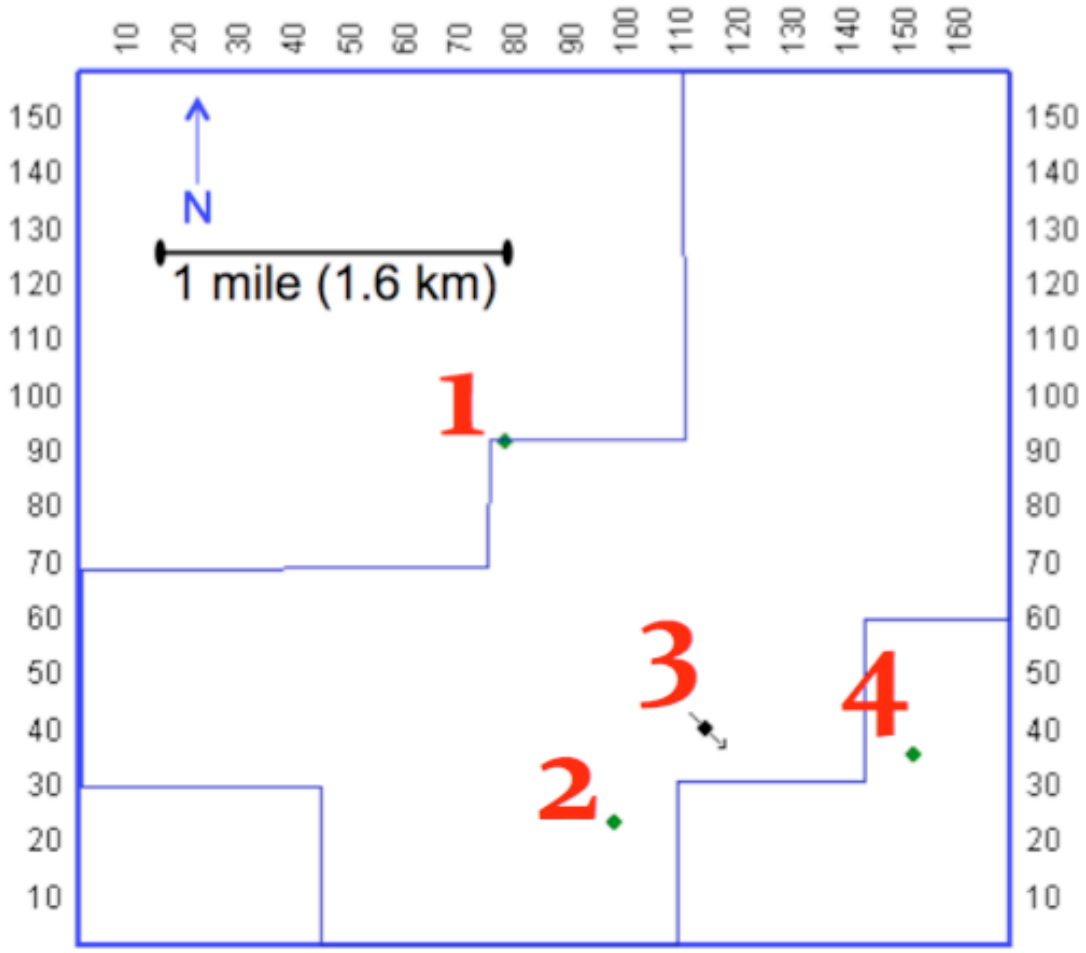

Figure 20. Deep penetrations in Dickman area and detail table.

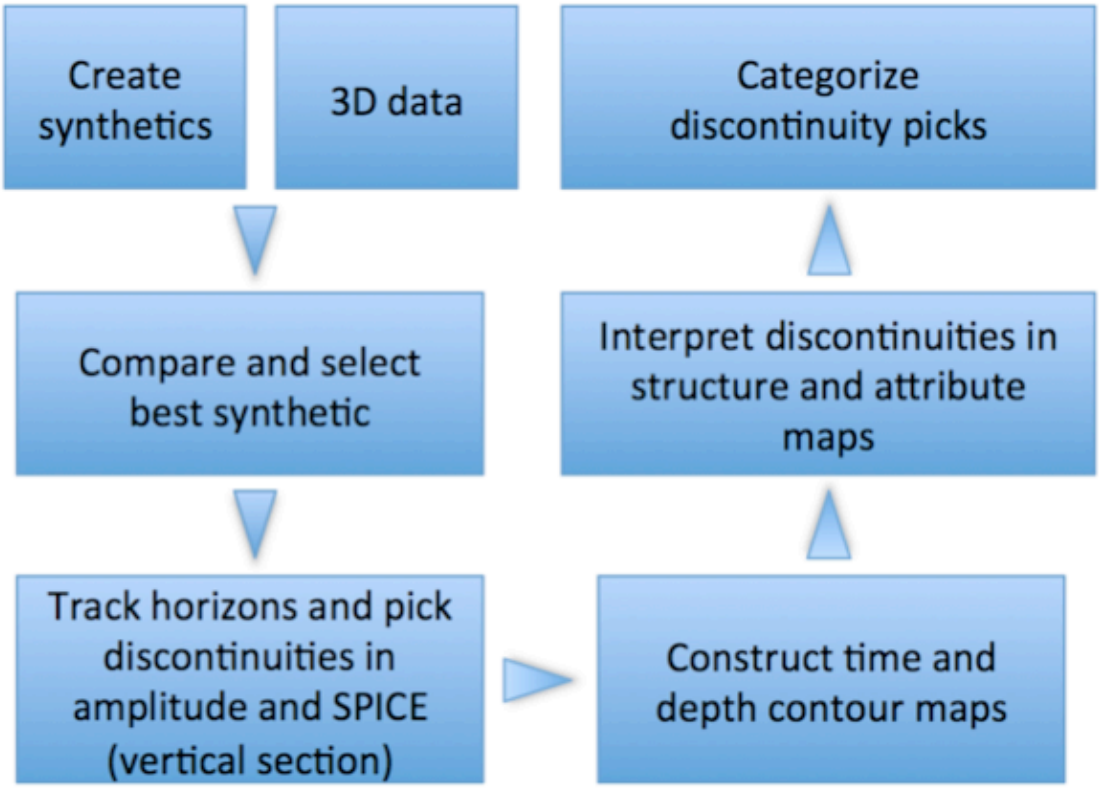

Figure 21. Deep structure mapping project workflow.

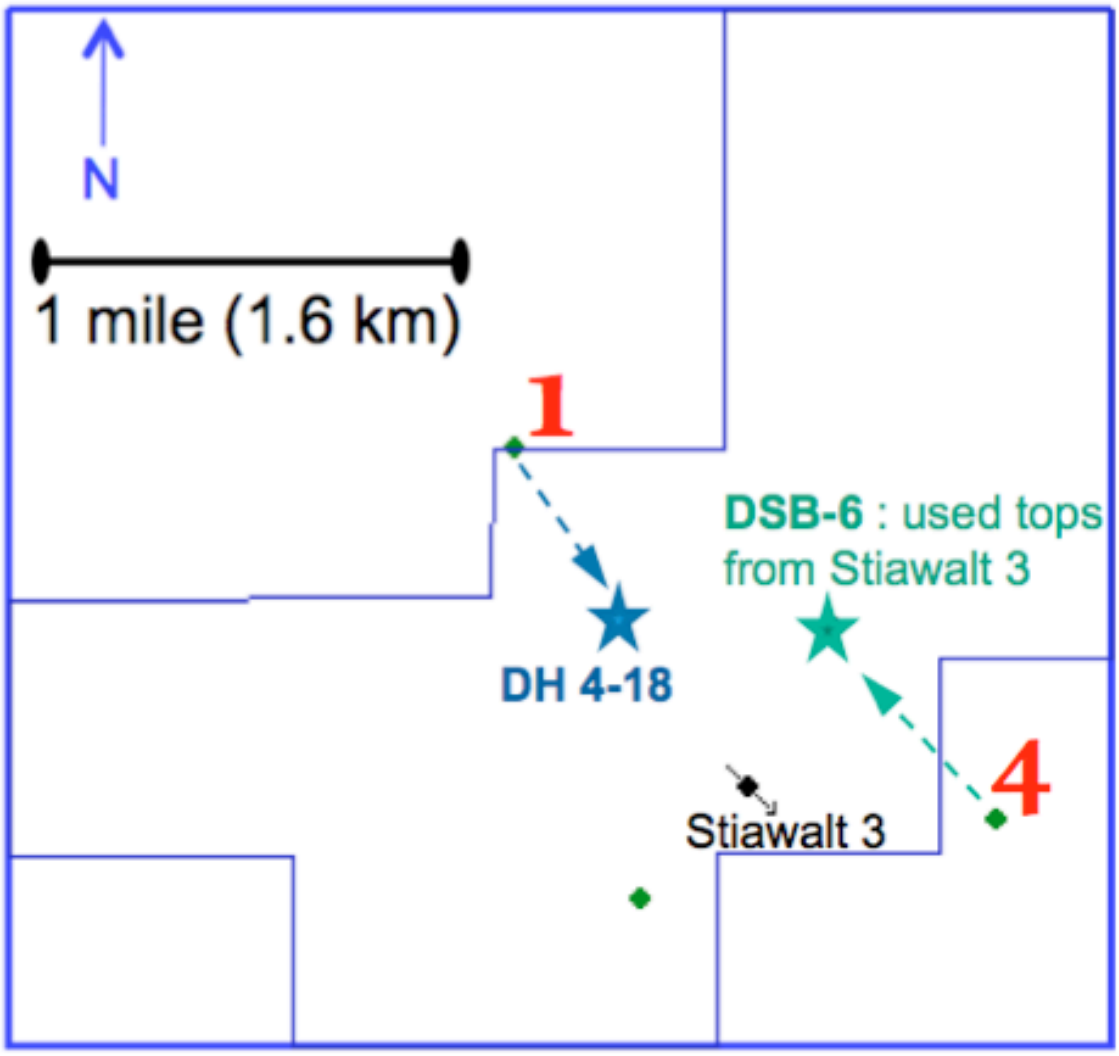

Figure 22. Dummy well locations.

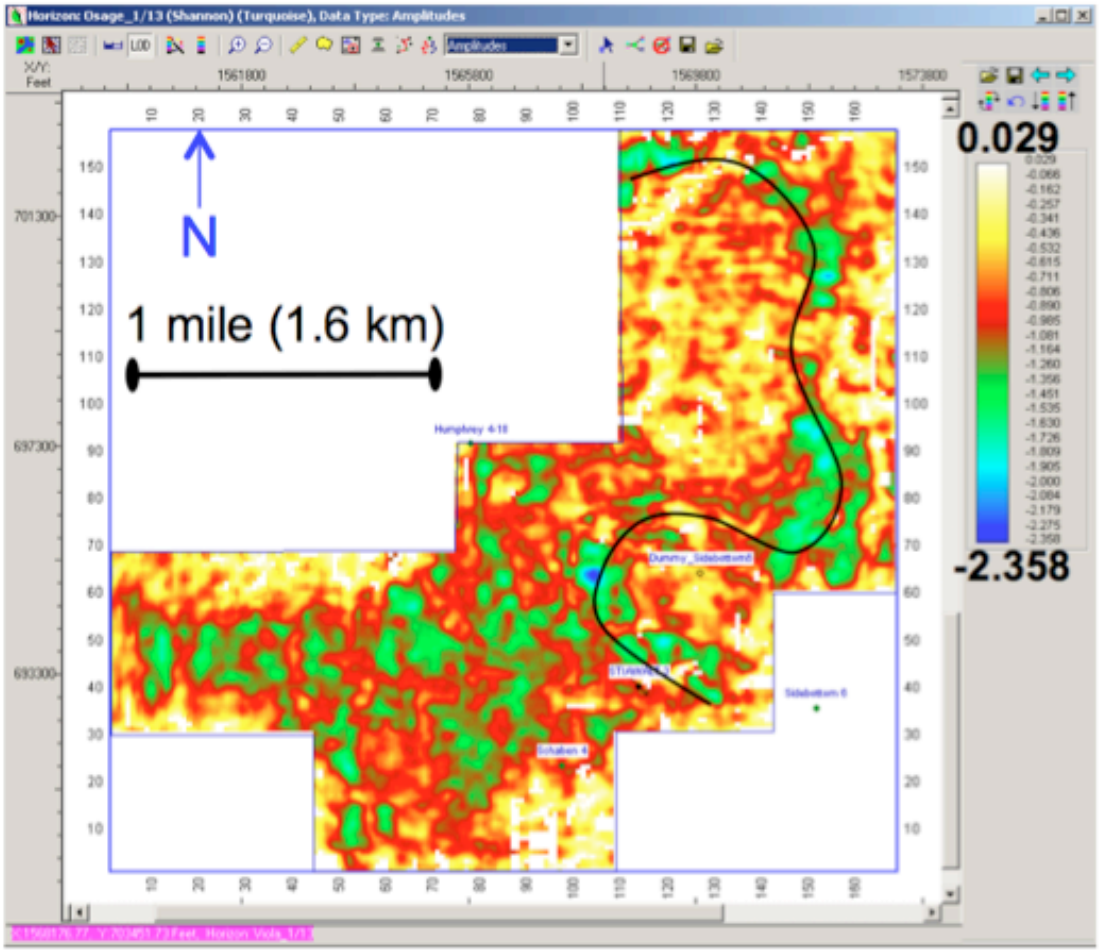

Figure 23. Osage amplitude map, note the highlighted channel.

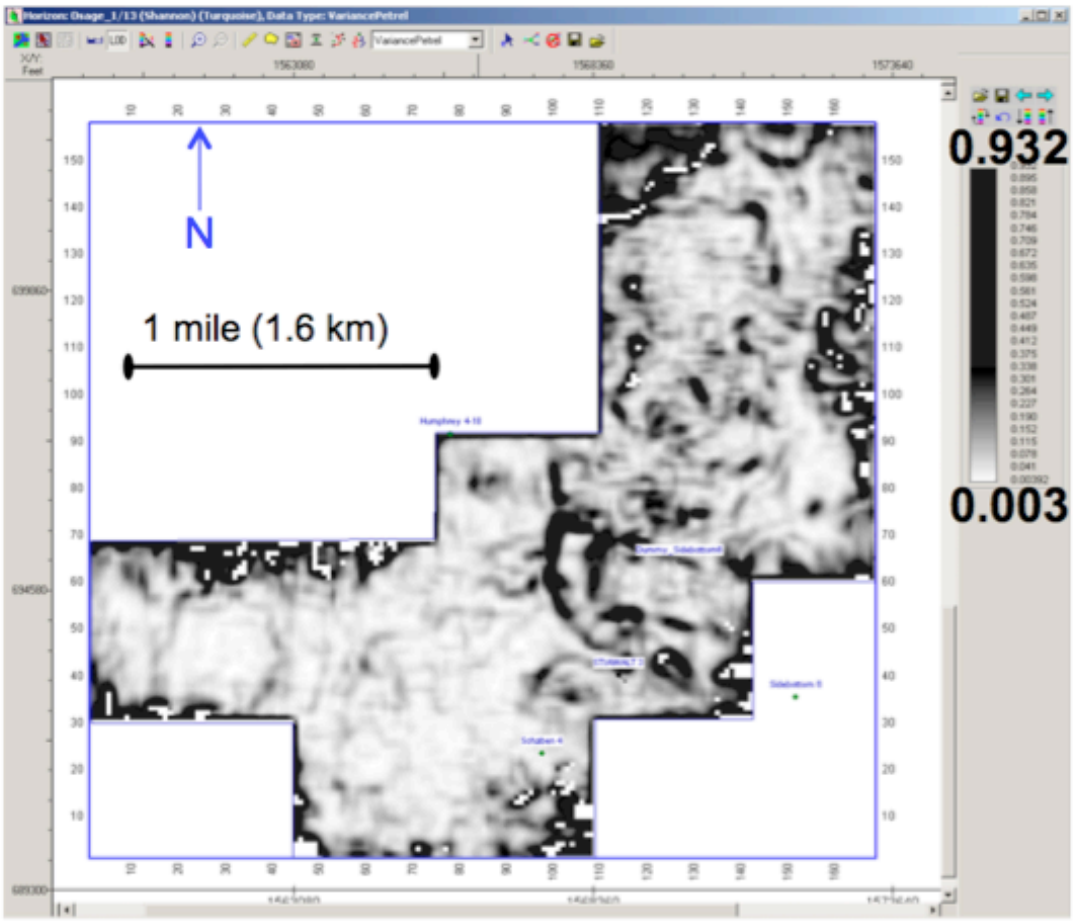

Figure 24. Osage variance map showing prominent channel feature.

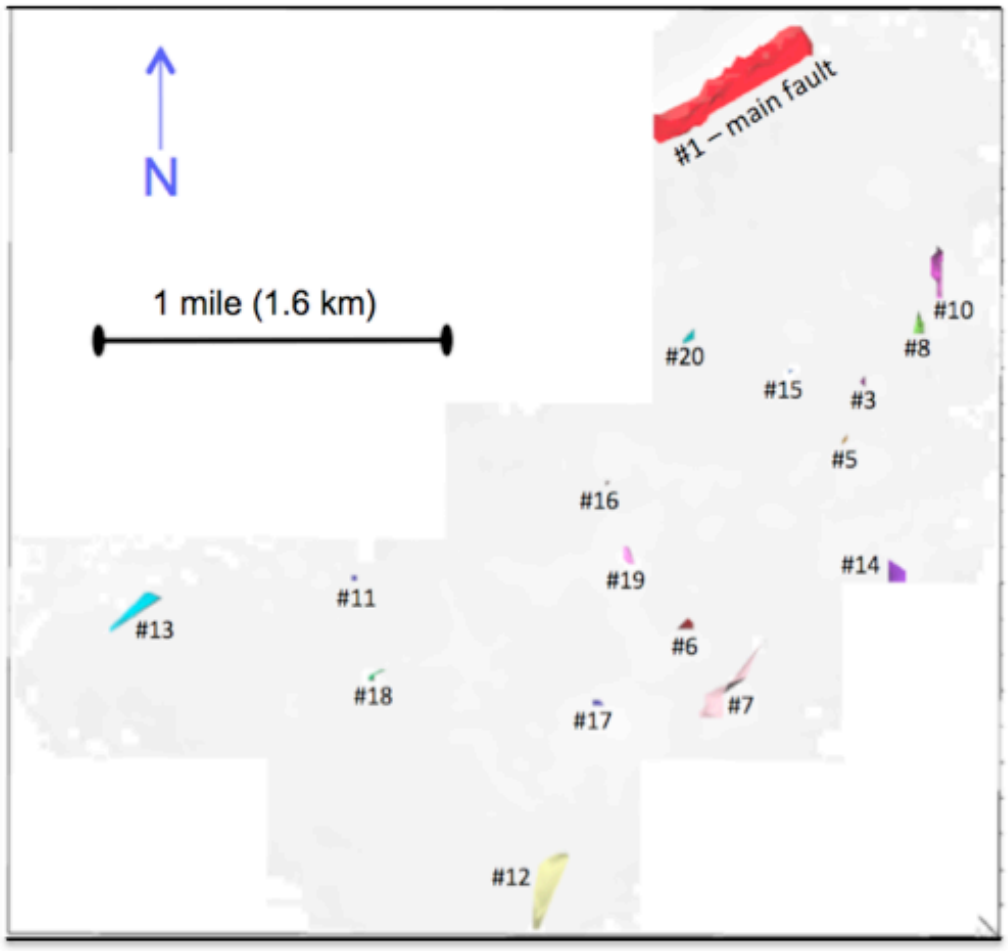

Figure 25. All fault/fracture picks (surfaces) displayed in darker color.

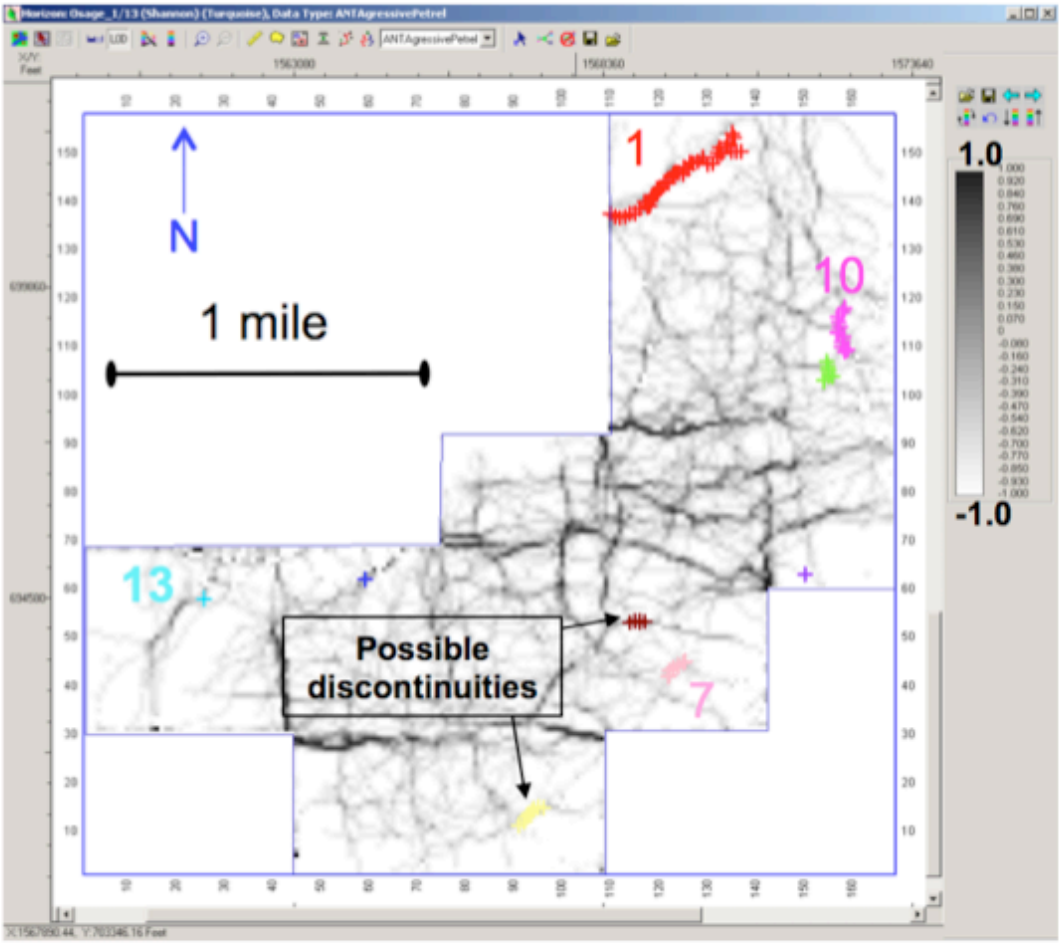

Figure 26. Osage ANT map with labeled probable fault.